Ultrasonics - Sonochemistry 67 (2020) 105122

Contents lists available at ScienceDirect

Ultrasonics - Sonochemistry

journal homepage: www.elsevier.com/locate/ultson

Optimization and characterization of zeolite-titanate for ibuprofen elimination by sonication/hydrogen peroxide/ultraviolet activity

Narges Farhadi[a], Taybeh Tabatabaie[a,*], Bahman Ramavandi[b,c,*], Fazel Amiri[a]

[a] Department of Environment, Bushehr Branch, Islamic Azad University, Bushehr, Iran
[b] Systems Environmental Health and Energy Research Center, The Persian Gulf Biomedical Sciences Research Institute, Bushehr University of Medical Sciences, Bushehr, Iran
[c] Department of Environmental Health Engineering, Faculty of Health and Nutrition, Bushehr University of Medical Sciences, Bushehr, Iran

ARTICLE INFO

Keywords:
Photo-catalyst
Ibuprofen
Titanium dioxide
Ultrasonic wave
Zeolite

ABSTRACT

In this study, a photo-catalyst of titanium oxide was coated on zeolite by the sol–gel method. The generation of the zeolite-titanate photo-catalyst was optimized at conditions of calcination temperature (300, 350, 400 and 500 °C), calcination time (1, 2, 3, and 4 h), and titanate content (0, 2, 4, 6, and 8 mL). The catalyst was used for 'Sonication/UV/H_2O_2" activity and finally, eliminating ibuprofen. Physicochemical properties of the as-built photo-catalysts for all optimized conditions were determined using FESEM-EDX-mapping, BET, FTIR, and XRD. The highest percentage of ibuprofen removal (98.9%) was obtained at conditions of zeolite to titanium ratio of 1 g: 2 mL, time in the furnace of 1 h, and temperature of the furnace of 350 °C. The optimum photo-catalytic (namely, Cat-350-1-2) had a surface area value of 39 m^2/g and a crystalline size of 4.9 nm. The surface area for all photo-catalysts increased after being used for ibuprofen removal, possibly due to ultrasonic waves. The presence of Ti-O, benzene ring, O-Al-O, O-Si-O, C–H, and O–H in the photo-catalysts structure were confirmed. Growing the calcination time resulted in an increase in the crystallinity of titanium dioxide in the photo-catalysts and, ultimately a reduction in the ibuprofen removal. The consumed energy by the developed system was calculated for the presence (0.094 kJ/g) and absence (17.5 kJ/g) of the ultrasonic wave. The degradation pathway and reaction kinetic are also explored and proposed. The results showed that the ultrasonic-UV-activated H_2O_2-based technique can be applied as an alternative method for ibuprofen removal from aqueous media.

1. Introduction

Emerging pollutants like personal care products, pharmaceuticals, and disruptive endocrine chemicals make a wide range of new contaminants in environmental matrices. These pollutants have caused recent ecological and health concerns. Pharmaceuticals comprise a wide range of therapeutic compounds that have been used in human and veterinary medicine for many years [1,2]. Ibuprofen (IBU) is usually prescribed for curing fever, inflammation, pain, or minor injuries. The worldwide consumption of IBU is ~ 200 tons per year. The presence of IBU can highly affect the growth of fish, microorganisms, seaweeds, and various fungal species. Ibuprofen affects estrogen homeostasis and thus damages reproduction [3]. Numerous studies have detected IBU in wastewater treatment plant effluents (0.002–95 μg/L), water bodies (0.01–0.4 μg/L), and tap water (0.00013–0.0002 μg/L) [4]. Finding this drug in the environment indicates the inability of conventional sewage treatment systems to remove it and also its stability in the environment. Therefore, it would be highly commendable to offer a technique that can remove or convert drugs like ibuprofen from wastewater to harmless compounds. Recent scientific papers have published several methods to eliminate IBU from aqueous media such as the adsorption to modified activated carbon [5,6], biodegradation [7,8], and advanced oxidation [9,10]. In the adsorption technique, the contaminant is only transferred from the water/ wastewater to the adsorbent structure without decomposition. Therefore, the proper disposal of saturated adsorbents is still an environmental concern. Biodegradation is also an excellent way to treat biodegradable pollutants. However, this method is not capable of entirely decomposing pharmaceutical compounds [11]. On the other hand, a lot of space is needed for this technique, so it is not economical [12]. One of the methods used in recent years to remove emerging pollutants is advanced oxidation-based methods. Advanced oxidation

* Corresponding authors at: Department of Environment, Bushehr Branch, Islamic Azad University, Bushehr, Iran (T. Tabatabaie); Systems Environmental Health and Energy Research Center, The Persian Gulf Biomedical Sciences Research Institute, Bushehr University of Medical Sciences, Bushehr, Iran (B. Ramavandi).
E-mail addresses: ttabatabaie@iaubushehr.ac.ir (T. Tabatabaie), b.ramavandi@bpums.ac.ir (B. Ramavandi).

https://doi.org/10.1016/j.ultsonch.2020.105122
Received 11 March 2020; Received in revised form 1 April 2020; Accepted 3 April 2020
Available online 04 April 2020
1350-4177/

processes are based on the generation of strong oxidants such as hydroxyl, sulfate, and chlorine radicals in solution. Hydroxyl radicals (OH ·) can quickly oxidize contaminants in a non-selective manner [13]. Photo-catalytic oxidation with ultraviolet-assisted radiation and semiconductor materials is a new approach for controlling organic compounds.

Among semiconductor materials, titanium dioxide is the most active photo-catalyst. Widespread use of this catalyst is due to its physical and chemical stability, low energy consumption, and cost-effectiveness, being non-toxic, and resistant to corrosion [14]. Stabilization of titanium dioxide nanoparticles on materials with an unusually high surface area increases the photo-degradation efficiency.

Research has shown that zeolites or their modified form can be used for oxidation processes [15]. The porous structure, morphology, and specific surface area of zeolites can affect their catalytic ability. One of the restricting aspects of the application of photo-catalysts is their low specific surface area. Modifying zeolites with metal oxides can provide a more active surface and prevent clotting, thus significantly enhancing the removal efficiency [16,17]. The TiO_2/zeolite catalyst is a new compound that can be tested in catalytic processes for pollutant removal.

Another component of advanced oxidation techniques is the sonication wave that has been used in processes such as sonolysis [18], sono-enzymatic degradation [19], sono-ozone process [20], sono-photo-catalytic process [9], sono-Fenton system [18], and sono-photo method [21]. The sonication wave can produce hydroxyl radicals and play a role in mass transfer [22].

The influence of inorganic oxidants, such as H_2O_2 to enhance the sono-degradation rate of pharmaceuticals, has been proven as a radical producer [21]. Hydrogen peroxide has advantages such as convenient storage and OH· oxidation power (K~10^6–10^9 M/s) by improving the O-O partition with quantum photon energy over other oxidizers like ozone, persulfate, and periodate [21]. Hydroxyl radicals are involved in purifying toxic organic compounds, eventually converting them into smaller compounds or carbon dioxide and water. Moreover, the hydroxyl radical is superior to the ozone oxidizer because ozone does not react with IBU [23].

The method of preparing and optimizing the factors affecting photo-catalyst construction is vital for achieving higher photo-catalytic activity. Three critical parameters for manufacturing photo-catalysts are TiO_2 loading, calcination temperature (time in the furnace), and calcination time (residence time in the furnace). The optimum values of the residence time of the material in the furnace and calcination temperature can develop the specific surface and cavity volume of the photo-catalyst and thus expedite the degradation rate [16].

Although some articles [24–27] have been published on zeolite/titanium to remove certain types of pollutants, the parameters that influence the construction of this photo-catalyst remain unknown and incomplete. Therefore, the purpose of this study was to optimize (I) furnace temperature, (II) furnace time, and (III) titanate to zeolite ratio to produce a zeolite/titanate photo-catalyst that has not yet been optimized and characterized so far. This photo-catalyst was used to remove ibuprofen in the 'zeolite/titanate/H_2O_2/sonication/UV' system. Physico-chemical properties of the prepared photo-catalysts are provided under different conditions. The mechanism, pathway, kinetics, and energy consumption for ibuprofen removal by the developed system were also explored.

2. Experimental

2.1. Materials, solutions, and devices

In this investigation, all chemicals were used without processing. Ibuprofen powder ($C_{13}H_{18}O_2$; 2-(4-isobutylphenyl)propanoic; solubility in water: 0.021 mg/mL at 20 °C; molecular weight: 206.29 g/mol, purity ≥98%) was purchased from Dana Pharmaceutical Company (Iran). Deionized water was provided by Zolal Chemical Medicine Company. Zeolite was purchased from Sigma and tetrapropyl *ortho*-titanate from Merck Company. Hydrogen peroxide was prepared from Kimia Exir (Iran) with a purity of 35%. Ethanol (96%) was also purchased from the Khorasan Distillery Company. NaOH and HCl were also bought from Kimia Materials Company and was used to adjust the solution pH. The stock solution of the ibuprofen molecule was prepared by dissolving the desired amount of IBU in distilled water. Due to the volatility of the stock IBU solution, it was prepared daily. Ultrasonic Model S30H from Elma Germany with 2.75 L capacity (tank inner dimensions of W: 240 mm, D: 137 mm, and H: 100 mm) and the frequency of 37 kHz and a UVC lamp (6 w, Philips, Poland). The amount of electrical energy coming into the reaction solution from the ultrasonic apparatus is calculated using the calorimetric method as 5.04 kJ. Other instruments used in this study included the furnace (Carbolite model), the oven (Shimaz model), the pH meter (Mettler Toledo), and the shaker-incubator (Fan Azmagostar model).

2.2. Reactor specifications

The cylindrical reactor was made of stainless steel with a height of 24 cm and a diameter of 4.1 cm with a volume of 460 mL. The UVC lamp was put into a quartz protective tube in the middle of the reactor. The volume of the reactor was reduced to 313 mL after installing the UVC lamp. During the tests, the reactor was placed inside the ultrasonic tank. The temperature was constant during the experiments through constant discharge water inlet and outlet in the ultrasonic device. Due to the limitation of the ultrasonic tank, half of the reactor (150 mL) was filled with IBU solutions. The schematic of the reactor is displayed in Fig. 1.

2.3. Optimization of zeolite-titanate photo-catalyst

The sol–gel approach was applied to make zeolite-titanate photo-catalysts [28]. To this end, 4 mL of titanium propoxide was added drop by drop to 2 mL of ethanol and agitated at room temperature for half an hour (Solution A). Then, 0.4 mL of nitric acid and 2 mL of distilled water were poured to 17 mL of ethanol (Solution B). After that, Solution B was added dropwise to Solution A and stirred for one hour until a clear sol was achieved. Then, 2 g zeolite was added to the transparent sol. The mixture was first agitated for half an hour and kept at room temperature (24 ± 1 °C) for 24 h. The ultimate solution was dried at 80 ± 2 °C for 4 h. The dried product was calcined for 3 h at 300 °C. Then, a photo-catalyst was obtained at 300 °C. The steps for preparing the zeolite-titanate photo-catalysts at temperatures of 350, 400, and 500 °C were repeated for 3 h. After cooling the samples, the zeolite-titanate photo-catalysts were powdered, sieved, and prepared for testing. The zeolite-titanate photo-catalyst was prepared at different incubation times and various ratio of zeolite to titanate. Reaction conditions for the optimization of the zeolite-titanium catalyst are fully described in Table 1.

2.4. Design of experiments

The amount of 15 mL of ibuprofen stock solution was taken and poured in the reactor. The volume of the solution was increased to 150 mL by the addition of distilled water and 0.7 mL of 35% H_2O_2 solution. The solution pH was set to 7 ± 0.2, then, 0.25 g of as-prepared catalyst was poured into the photo-reactor. The reactor was placed in the ultrasonic bath apparatus for 100 min. After the desired time, the content of the reactor was passed through the filter (Whatman paper, 0.42 μm) and the residual of IBU and COD parameter of the filtrate was analyzed. In this study, all experiments were repeated three times, and the mean of the acquired results is presented alongside the standard deviation (as error bars in the figures). The efficiency of the measurements was calculated based on the material balance formula.

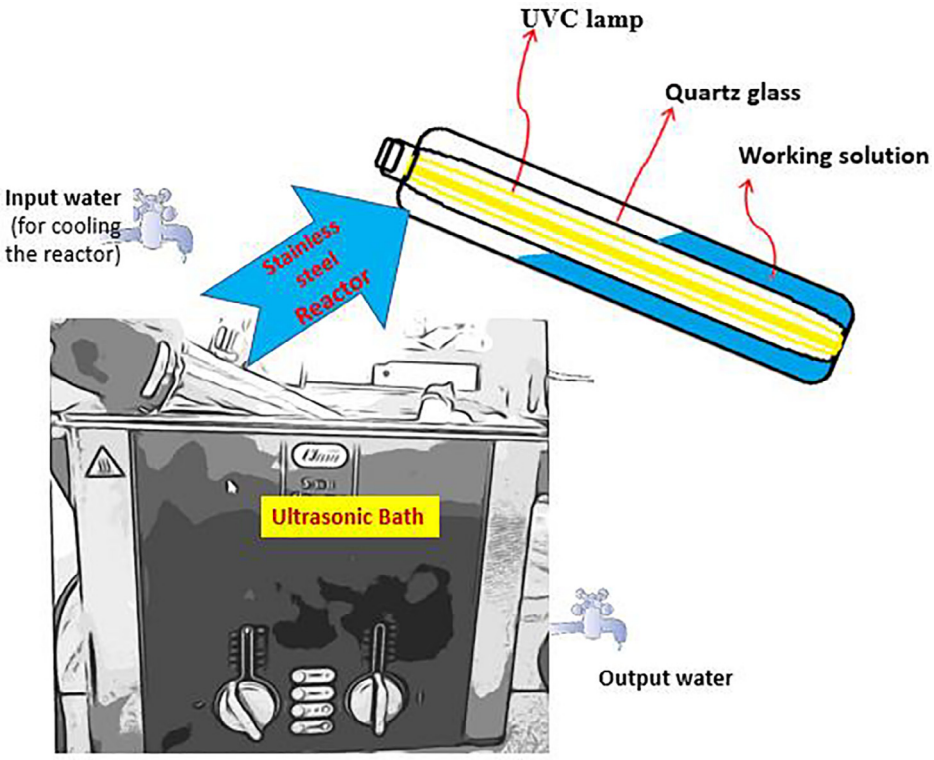

Fig. 1. Schematic of the reactor and accessories used in this research.

2.5. Measurements

To characterization purposes, the used photo-catalysts were separated by the filter and dried at 70 °C for 5 h. SEM-mapping, FTIR, EDX, BET, and BJH experiments were performed on the dried samples. The same tests were performed for the fresh photo-catalyst. The surface morphology of the zeolite-titanate materials was determined by FESEM using the German Zeiss Sigma VP Electron Microscopy Scanner. The samples were subjected to a high vacuum with a thin layer of gold for electrical conductivity in a sputtering system. The specific surface characterizations of the photo-catalyst samples were done using an automated BET analyzer (Micrometric, Model ASAP 2020) by measuring nitrogen adsorption at 77 K. In this method, by measuring the pressure of nitrogen injected into the interior of the materials, the specific adsorption surface is analyzed. Functional groups were analyzed using Fourier Transmission Infrared (FTIR, Bruker-Germany Tensor Model II), in the range of 400–4000 cm^{-1}. To describe the crystal structure, X-ray diffraction (XRD, Pert Pro 'X, a Panalytical company) patterns were performed on an advanced D8 X-ray diffractometer with Cu Kα at 40 kV and 40 mA from 5 to 80° (2θ) and recorded using a detector. The chemical composition was evaluated simultaneously by EDX and mapping experiments using Oxford Instrument UK. The COD measurements were performed using the HACH spectrophotometer DR6000 using a photometer at 620 nm after the removal of the confounders. The content of the IBU molecule was determined by Waters 2695 HPLC tool equipped with a specified detector (Waters Alliance 2998-PDA) at λ = 210 nm. The mixture of formic acid (0.1%) and methanol (25:75 v/v), pH 2.5, at a flow rate of 1.0 mL/min was applied as an eluent.

3. Results and discussion

3.1. Effect of furnace temperature on ibuprofen removal

Fig. 2 shows the effect of the furnace temperature on the removal rate of ibuprofen. In the first step, for the manufacturing of zeolite- TiO_2 photo-catalyst, the effect of different calcined temperature (300, 350, 400, and 500 °C for 3 h) was investigated. As shown in Fig. 2, the highest percentage of ibuprofen removal (COD: 68% and IBU: 78%) was obtained with the Cat-350-3-4 photo-catalyst. The calcination temperature for each photo-catalyst directly affected on its crystallization and photocatalytic activity. Heating of TiO_2 at high temperatures causes its irreversible change; for example, the yellowing (burning) of titanate due to the development of the crystal lattice and the band reconstructed by the growth of rutile nuclei and crystalline formation [29]. The above factor results in a decrease in the specific surface of TiO_2 and thus results in weaker photo-catalytic activity. Calcination has not been tested at high temperatures. Because at temperatures > 600 °C the rutile phase of titanate dominates, which reduces its photovoltaic activity [30]. The catalyst synthesis method is one of the main factors affecting the physical and chemical properties. Generally, the high temperature reduces the surface area of TiO_2 and decreases the level of

Table 1
Test conditions for optimization of the zeolite-titanium catalyst for removal of ibuprofen (catalyst dose: 1.5 mg/L, sonication time: 100 min, and ibuprofen concentration: 100 mg/L).

Parameter	Furnace temperature (°C)	Residence time in furnace (h)	mL titanate: 2 g zeolite	Catalyst name
Effect of furnace temperature	300, 350, 400, 500	3	8:2	Cat-350-3-4
Effect of residence time in furnace	350	1, 2, 3, 4	8:2	Cat-350-1-4
Effect of titanate: zeolite ratio	350	1	0:2, 4:2, 8:2, 12:2, 16:2	Cat-350-1-2

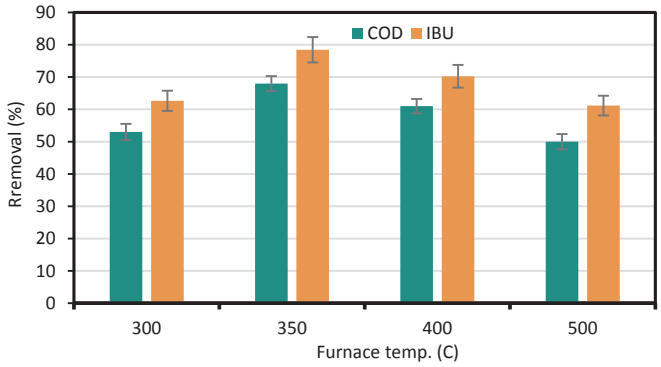

Fig. 2. The percentage removal of ibuprofen by zeolite-titanate catalyst prepared at different temperatures (solution pH: 7 ± 0.2, H_2O_2 concentration: 0.7 mL, sonication time: 100 min, catalyst dose: 150 mL).

hydroxyl groups [31]. In a study [28], the sulfadiazine adsorption and degradation efficiency by titanium zeolite catalyst decreased with increasing calcined temperature from 450 °C (93%) and 800 °C (86%). A little decline in the percentage of pollutant decomposition could be due to the increase in the particle size and crystallinity of TiO_2. Higher furnace temperatures yield larger TiO_2 crystals on the zeolite surface and subsequently reduces the removal efficiency [32]. The results show that the furnace temperature can notably impact on the physical characteristics of TiO_2 [33]. As the calcination temperature increases, the specific surface area decreases due to the crystalline extension of TiO_2 [34]. In the case of the zeolite-titanate photo-catalyst prepared at 350 °C showed the highest BET surface area. This results in more photo-catalytic catalytic activity for the removal of pollutants. It is also reported that the activation of the carbon-manganese catalyst increases at 400 °C due to the synergistic effect of the crystallized ions and the appropriate phase composition [35].

3.2. Influence of furnace temperature on properties of Cat-350-3-4

3.2.1. Bet

Fig. S1 displays the adsorption–desorption isotherm of nitrogen and particle size distribution for the Cat-350-3-4 photo-catalyst before and after the usage as an activator of H_2O_2/UV/Sonication. According to the IUPAC denomination, this catalyst is belonged to type I and IV Langmuir adsorption (which corresponds to the typical adsorption graph for mesoporous material) and has an H3 hysteresis ring at high pressures. For this type of hysteresis, the shape of cavities is a combination of layers and cylindrical. The adsorption capacity increased with increasing relative pressure due to the adsorption of N_2 multilayers in the inner surface of the mesopores. The rapid increase in adsorption capacity caused a sudden change in the relative pressure between 0.95 and 1 due to the N_2 capillary density. The BET surface area of fresh and used Cat-350-3-4 was computed to be 127 m^2/g and 205 m^2/g, respectively. Increasing the surface area of the photo-catalyst after being used in the IBU removal process indicates the formation of some new cavities or the conversion of some micro- to meso-cavities during the reaction. Another plausible reason for the increase in the surface area could be the breakdown of photo-catalyst particles by ultrasonic waves (and the creation of new surfaces). According to Table 2, the diameters of the Cat-350-3-4 cavities before and after used in the reaction solution are equal to 9.6 nm and 4.5 nm, respectively. The cavities' diameter of the photo-catalyst decreased after being used, indicating its effective activity in reducing the target contaminant [36].

3.2.2. Ftir

The FTIR test was performed to investigate the functional groups and the impact of furnace temperature on zeolite-titanate formation. The FTIR spectrum of the Cat-350-3-4 sample is shown in Fig. S1. First, each spectrum is normalized to the maximum transmittance of the same spectrum and then plotted. As shown in Fig. S1, six peaks are visible at wavelengths less than 1700 cm^{-1}. Wide bands at 3100–3700 cm^{-1} due to OH stretching of water (H_2O) or surface hydroxyl groups on TiO_2 which play a critical role in the photo-catalytic reaction. Because the mentioned groups can prevent the reproduction of photovoltaic loads and therefore, the reaction does not stop with the presence of these oxygenated functional groups [35]. It can be traced that the peak intensity of these two groups increases with increasing calcined temperature. This issue reduces the photo-catalytic efficiency of zeolite-TiO_2 [37]. The small peak appearing at 1631 cm^{-1} is affiliated to the bending vibration of O–H groups in the zeolite structure [38]. The peaks visible at the wavenumbers of 1174 cm^{-1}, 1046 cm^{-1}, and 905 cm^{-1} are related to the flexural vibration of the CH bond, the tensile vibration of O-Si-O [39], and the tensile vibration of the Si-O-Al bond, respectively. It is observed that the wavenumbers of these bonds remain approximately unchanged after ibuprofen removal. The peak visible at the wavenumber 700 cm^{-1} to 800 cm^{-1} is the tensile vibration of bonds in the benzene ring [40]. As can be seen, the wavenumber for this peak decreased after IBU catalytic removal. This indicates the successful adsorption of this pollutant on the catalyst surface. The broad peak is also visible at wavelengths less than 800 cm^{-1} belongs to titanium oxide bonds which confirm the presence of titanate in the photo-catalyst [41].

3.2.3. Xrd

The structure of the zeolite-titanium photo-catalyst before and after use in the ibuprofen removal was examined by XRD test. The acquired findings are shown in Fig. S1. The modification of the zeolite structure by TiO_2 can be confirmed by this test. The XRD pattern of natural zeolite at $2\theta = 25^{\circ}$ has peaks that match the peaks expressed in the reference codes. By comparison of the photo-catalyst before and after the contaminant removal, it can be seen the peak of TiO_2 in the catalyst structure. This confirms the success of high TiO_2 loading on zeolite. At furnace temperature of 350 °C, Cat-350-3-4 showed the highest photo-catalytic activity which further confirms that calcined temperatures can affect the properties of zeolite and titanate. As shown in Fig. S1, the two XRD spectra before and after being used for the ibuprofen oxidation have approximately identical peaks. By matching the two spectra to the reference spectra, titanium oxide (reference code: 01-073-1764) known as anatase and zeolite (reference code: 01-085-1686) are identifiable, where the anatase phase is predominant. By comparison of two XRD spectra for before and after pollutant removal, it was observed that the intensity of the spectral peaks (especially the peak of $2\theta = 25$) is reduced. The decrease in the crystalline peak intensity of the used photo-catalyst may be due to the formation of a complete coating of IBU molecules on the catalyst surface. The absence of specific peaks for TiO_2 indicates that the titanate particles are suitably dispersed on the zeolite which inhibits further growth of TiO_2 crystals [42]. It has also been found that calcination temperature affects the photo-catalytic activity of calcined samples [11]. A researcher has stated that if the catalyst preparation temperature elevated, the intensity of the XRD peaks would decrease, resulting in a decrease in crystallinity and peak width and an increase in the crystal size [28].

3.2.4. FESEM-edx

According to Fig. 3, elements of silicon, oxygen, and aluminum are present in the fresh Cat-350-3-4 catalyst structure. The presence of titanium proves the presence of anatase in the system as confirmed by the XRD test. The results of the elemental surface analysis of the used Cat-350-3-4 catalyst are also shown in Fig. 3. After the catalytic reaction, in addition to the preceding elements, the carbon content in the catalyst has increased substantially. This indicates the successful removal of IBU by the developed system (sonication/UV/H_2O_2/photocatalyst). In Fig. 3, it is clear that the used photo-catalyst has been reacted with the contaminant. It is also clear that the mean size of the nanoparticles is

Table 2
The most important properties of photo-catalysts prepared from zeolite-titanate for ibuprofen removal.

Parameter	Unit	Cat-350-3-4		Cat-350-1-4		Cat-350-1-2	
		Fresh	Used	Fresh	Used	Fresh	Used
BET	m^2/g	127	205	96	110	39	110
BJH desorption cumulative surface area of pores	m^2/g	132	220	99	105	18	80
Adsorption average pore width (4 V/A by BET)	nm	5.5	3.4	6.2	5.0	7.5	6.2
BJH adsorption average pore diameter (4 V/A)	nm	9.6	4.5	11.6	9.7	54.8	12.0
BJH desorption average pore diameter (4 V/A)	nm	8.7	4.3	10.5	8.7	40.4	11.1
Crystal size	nm	8.4	6.0	8.8	6.6	8.5	4.9

about 35 nm. The smaller the particle reflects the lower the calcination temperature. EDX tests were used to examine more accurately the quantities of ibuprofen removal by the system (Fig. 3). After coating the zeolite with the TiO_2 surface, the surface of the catalyst is smoothed, indicating that the TiO_2 particles are insoluble in the zeolite and block the pores to some extent. In the meantime, some fine particles are

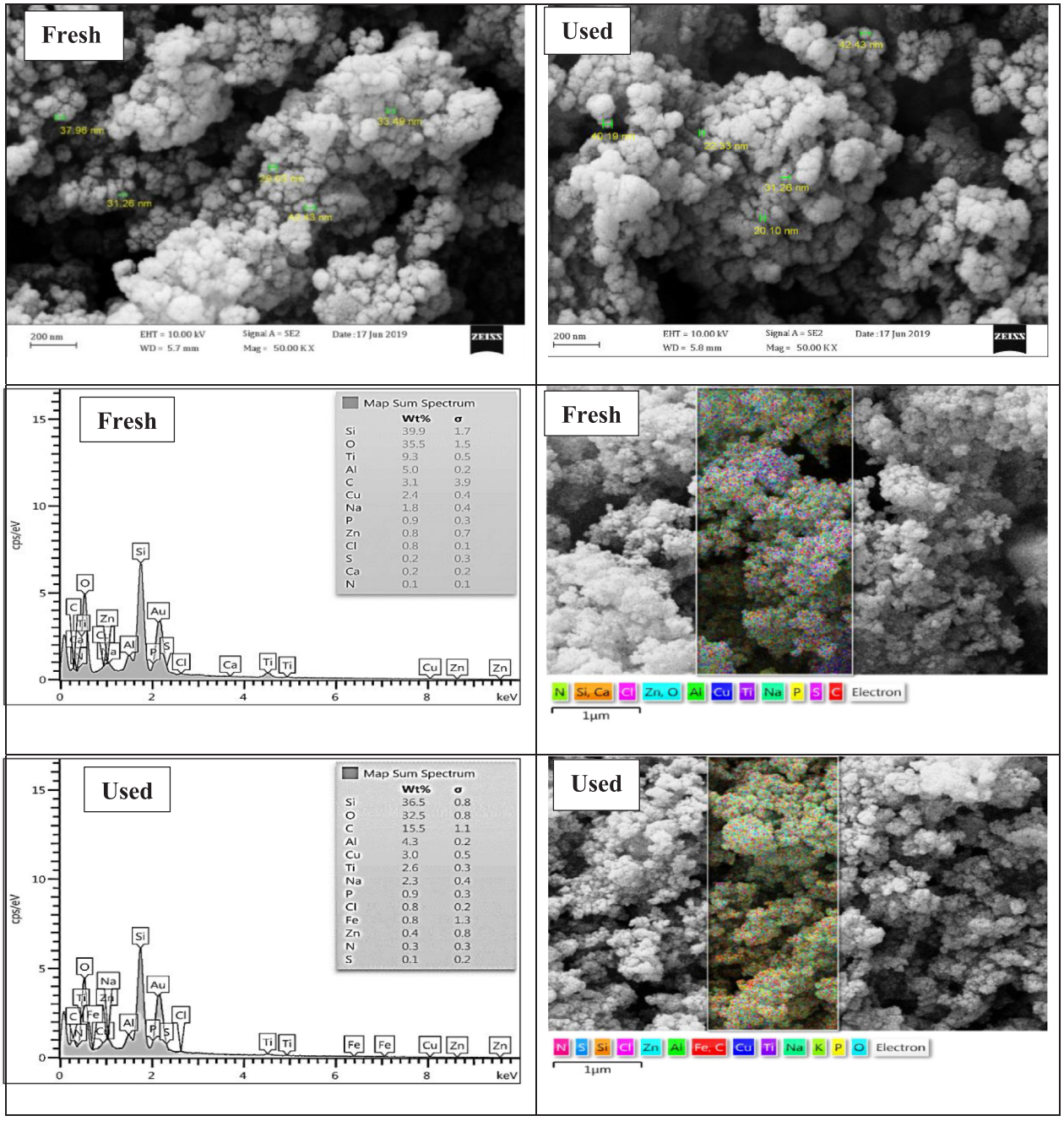

Fig. 3. SEM, EDX, and mapping for the fresh and used Cat-350-3-4 catalyst.

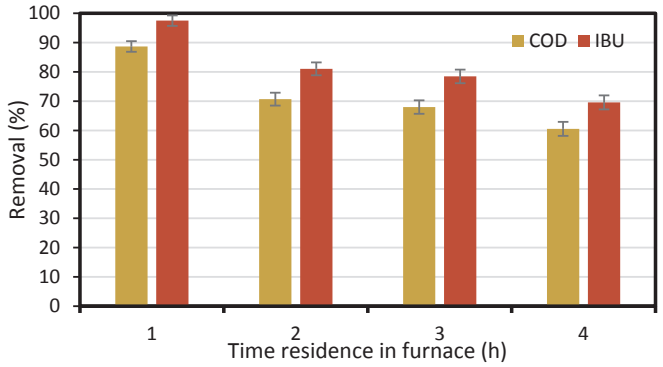

Fig. 4. The percentage removal of ibuprofen by zeolite-titanate catalyst prepared at different time residence in the furnace (solution pH: 7 ± 0.2, H_2O_2 concentration: 0.7 mL, sonication time: 100 min, catalyst dose: 150 mL).

observed around the zeolite-TiO_2. A portion of the TiO_2 particle does not precipitate in the inner pores and is dispersed on the surface of the zeolite. After the TiO_2 stabilization, the particle agglomeration is attenuated and showed a certain dispersion. The TiO_2 particles have a grain distribution on the zeolite surface with a size of 25–45 nm. According to the results of the EDX test, it is also found that in the used photo-catalyst, the weight percent of the zeolite constituents (silicon and oxygen) decreased. In contrast, the percentage of carbon at the catalyst surface increased. This could indicate the creation of a layer of IBU on the catalyst surface.

3.3. Influence of the residence time in furnace on the removal of ibuprofen by photo-catalyst

Fig. 4 displays the effect of the photo-catalyst incubation time in the furnace on the removal rate of ibuprofen. As can be seen, the Cat-350-1-4 photo-catalyst has the highest removal efficiency of 88.67% (based on COD) and 97.5% (based on IBU) for 1 h furnace time, whereas the removal rate was about 68% (based on COD) for 3 h furnace time using Cat-350-3-4. As the photo-catalyst stays longer in the furnace, the removal efficiency is reduced. Other studies have shown that calcination at very short times leads to incomplete crystallization and long-time cause redness and burns of TiO_2 [43].

3.4. Influence of furnace residence time on properties of Cat-350-1-4

3.4.1. Bet

Fig. S2 illustrates the adsorption–desorption isotherm of nitrogen by the Cat-350-1-4 photo-catalyst. The isotherm is a mixture of type IV and V for both fresh and used catalysts. Having an H3-type hysteresis ring at high pressures of $p/p^{\circ} = 0.5–0.95$, indicating mesoporous structure which resulted in condensation of capillaries. The accumulation of crystals causes meso-crystalline spaces in the form of meso-cavities. The structure of the cavities is of complex mesoporous type and these rings belong to porous minerals.

As shown in Table 2, the BET specific area of pristine Cat-350-3-4 and Cat-350-1-4 catalysts was 127 m^2/g and 96 m^2/g, respectively. In the second step of the photo-catalyst optimization, the BET value was reduced. This refers to the length of time the catalyst stayed in the furnace, which may have affected the size of the crystals. According to Table 2, the pore diameter for the fresh Cat-350-3-4 and Cat-350-1-4 was 9.6 nm and 11.6 nm and the used ones were reached to 4.5 nm and 9.7 nm, respectively. For the second optimization step (Cat-350-1-4), the diameter and volume of the cavities increased. The higher pore volume provides better contact between the catalyst and IBU and ultimately has a significant impact on its removal rate by sonication/UV/H_2O_2 [44,45].

3.4.2. FT-Ir

The FT-IR spectra of the Cat-350-1-4 samples are shown in Fig. S2. In Fig. S2 the same six absorption peaks plus two small ones are visible. Two peaks visible at the wavenumbers of 2880 cm^{-1} and 2980 cm^{-1} are related to the symmetric and asymmetric tensile vibrations of the C–H bonds. The peak located at the 1394 cm^{-1} wavenumber corresponds to the flexural vibration of the CH_2 bond. The observation of these peaks could be implied the removal of IBU molecule by the photo-catalyst. After IBU oxidation, the O-Si-O peak intensity was decreased in the catalyst, which may be due to the coating of the zeolite-titanate with the contaminant. For the used photo-catalyst, the peak of the benzene ring was intensified. This is another confirmation of the successful removal of ibuprofen (containing benzene ring) by the system.

3.4.3. Xrd

The XRD spectrum for the Cat-350-1-4 photo-catalyst is presented in Fig. S2. As is depicted in this figure, the crystal peaks appear in the same positions to that of in Fig. S1, indicating the presence of zeolite and titanium oxide (anatase) compounds in the catalyst structure. The decrease in crystal peak intensities (especially the higher ones) in the used photo-catalyst samples indicates the treatment of ibuprofen by sonication/UV/H_2O_2/photo-catalyst. As shown in Fig. S2, the 1 h calcination time sample (Cat-350-1-4) had the greatest effect on the IBU removal by the zeolite-titanate catalyst.

3.4.4. FESEM-Edx

To investigate the effect of the Cat-350-1-4 catalyst on ibuprofen elimination the corresponding FESEM images (for pre- and post-usage) are shown in Fig. 5. Given this figure, the agglomeration of the catalyst grains is evident before and after using the photo-catalytic process. The results of the elemental analysis of the catalyst (Cat 350-1-4) surface are also shown in Fig. 5. Again, the presence of silicon, oxygen, and aluminum proves the existence of the zeolite structure and the trace of titanium is the reason for the presence of TiO_2 in the photo-catalyst, which was proved by XRD test. The results of surface elemental analysis of used Cat-350-1-4 are illustrated in Fig. 5. An approximately two-fold increase in the percentage of carbon element on the catalyst surface as well as a significant decrease in the percentage of titanium element confirms that the catalyst surface is covered by a layer of contaminants, confirming the successful treatment of ibuprofen by the system.

3.5. Influence of titanate to zeolite ratio on ibuprofen removal

The effect of loading amounts of titanate on zeolite on IBU removal is shown in Fig. 6. As can be seen, the percentages of COD removal by Cat-350-1-2, Cat-350-1-4, and Cat-350-3-4 are 89%, 88.67, and 68%, respectively. There was no significant difference between the results of the catalyst removal rates of Cat-350-1-2 and Cat-350-1-4. Therefore, Cat-350-1-2 was preferable in terms of economics and physicochemical properties. The lower the titanate content, the higher the removal efficiency of the contaminant. Increasing TiO_2 loading creates a linear reduction in specific surface area which may be due to precipitation of TiO_2 particles at the zeolite surface and pore blockage. Increasing TiO_2 content in the TiO_2/ HZSM-11 catalyst from 3 to 30 wt% continuously increases photocatalytic activity, but higher values decrease efficiency [32]. This may be due to the generate large TiO_2 particles on the zeolite surface, which confirms the results of this study.

3.6. Influence of titanate to zeolite ratio on properties of Cat-350-1-2

3.6.1. Bet

Fig. S3 shows the nitrogen adsorption–desorption isotherms for the third step of photo-catalyst optimization (Cat-350-1-2). According to the IUPAC classification, isotherms of the fresh and used photo-catalyst exhibited the type III and IV with an H3 type hysteresis ring. The BET surface of the Cat-350-1-2 sample was significantly increased after

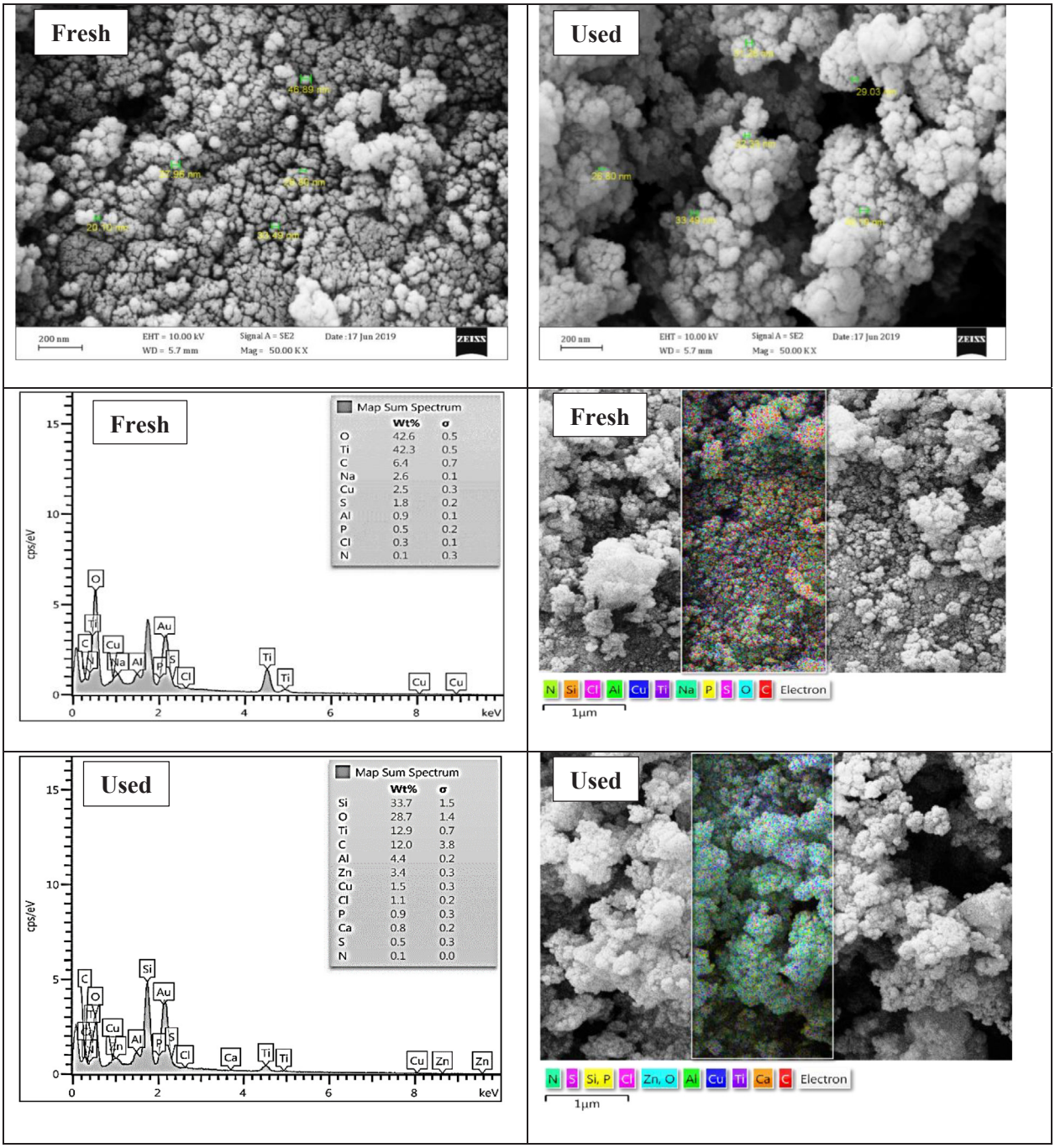

Fig. 5. SEM, EDX, and mapping for the fresh and used Cat-350-1-4 catalyst.

being used in the reaction mixture. Again, the main reason for this may be the use of sonication during the ibuprofen removal process. The pore structure factors, as opposed to BET areas, were significantly reduced. Because the deposition of TiO_2 on the zeolite surface will block the pores. The TiO_2 particles cover not only the surface of the zeolite but also the pores. That is the plausible reason behind the higher removal efficiency of ibuprofen by Cat-350-1-2 than that obtained by Cat-350-1-4. On the other hand, when the amount of TiO_2 is slightly increased, the accumulation at the zeolite surface increases. As a result, the particle size increases, the dispersion decreases, and ultimately the photocatalytic activity decreases. A previous study reported that catalyst samples containing 30% calcined TiO_2 at 450 °C have the best performance [32]. This study demonstrated the best performance of a sample containing 2 mL titanate at a calcined temperature of 350 °C

3.6.2. FT-Ir

The FT-IR spectra of the samples were incubated at 350 °C for 1 h in the presence of 2 mL of titanate (Cat-350-1-2) are depicted in Fig. S3. The two FTIR spectra for the pre- and post-pollutant removal are almost identical. But the peak resonance due to the flexural vibration of CH_2 indicates the successful removal of the IBU molecules by the zeolite-titanate surface.

3.6.3. Xrd

The XRD spectra of the Cat-350-1-2 photo-catalyst (before and after the reaction with IBU) are visible in Fig. S3. Like the result of the FT-IR test, no specific change in the XRD spectrum was observed for both pre- and post-used samples. Three diffraction peaks were observed in the zeolite-titanate catalyst at 2θ values of 25.5°, 37.9°, and 48.2°, which

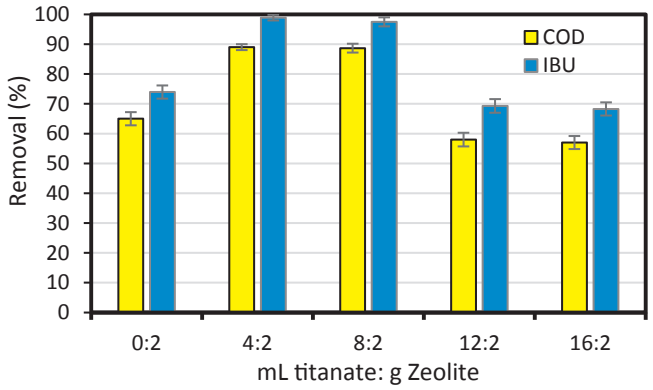

Fig. 6. The percentage removal of ibuprofen by zeolite-titanate catalyst prepared with different ratios of zeolite: titanate (solution pH: 7 ± 0.2, H_2O_2 concentration: 0.7 mL, sonication time: 100 min, catalyst dose: 150 mL).

represents (1 0 1), (0 0 4), and (2 0 0) TiO_2 anatases, respectively. The XRD analysis affirmed the successful incorporation of TiO_2 by the zeolite plates. As shown in Fig. S3, the diffraction peak has not changed in the samples. This structure may have two properties: First, the presence of TiO_2 particles does not affect the zeolite structure and second, TiO_2 and zeolite have synergistic effects [28]. As shown in Fig. S3, the widening of the peaks in the presence of less titanate means a decrease in the crystalline size of the titanium oxide. The crystallite size was calculated by the following formula:

$$D = K\lambda/B\cos(\theta) \quad (1)$$

where λ is the x-ray wavelength used (1.54 Angstrom), K is the shape factor (approximately 0.9), B is the peak width at half-height, and θ is the peak location. Decreasing the crystallinity of nanoparticles may increase the amount of contaminant adsorption. The crystallite size of titanium oxide in samples containing 4 mL and 2 mL of titanate approximately was computed to be 6.63 nm and 4.97 nm, respectively. Therefore, it can be concluded that the decrease in the amount of titanate reduced the crystallite size of TiO_2 particles. Reducing the size of the crystals results in a higher dispersion of the TiO_2 particle on the zeolite surface and thus a higher removal efficiency. The decrease in the crystallinity of nanoparticles may be due to increased contaminant removal [28].

3.6.4. FESEM-Edx

The morphology of the Cat-350-1-2 catalyst was determined by FESEM analysis. Fig. 7 shows prismatic crystals property of zeolite and spherical TiO_2 nanoparticles (20–45 nm) and clusters linked to the surface of the used and fresh zeolite-titanate. As shown in Fig. 7, the presence of silicon, oxygen, and aluminum prove the presence of the zeolite structure. Also, the detection of titanium confirms the presence of TiO_2 in the developed catalyst. The amount of carbon can indicate whether or not the ibuprofen reacts with the catalyst surface. Here, it is observed that before the reaction, the amount of carbon element is meager at about 1%. After the removal process, a 9-fold increase in carbon content and a decrease in the titanium percentage of the photocatalyst structure has happened. However, ultrasonic waves have also contributed to the high accumulation of carbon compounds on the catalyst surface by accelerating mass transfer. These issues may be an indication of the successful removal of IBU by the developed process.

3.7. Effect of presence/absence of ultrasonic wave on the IBU removal kinetic

The kinetics of ibuprofen decomposition in the presence (Zeolite-TiO_2-UV/Ultrasound/H_2O_2) and absence of ultrasonic waves (Zeolite-TiO_2-UV/H_2O_2) were investigated. The pseudo-first-order equation was used to determine the kinetics rate (Eq. (2)). The corresponded results are depicted in Fig. 8.

$$\ln\left(\frac{IBU_t}{IBU_0}\right) = -k.\ time \quad (2)$$

The rate of removal of ibuprofen (k, 1/min) in the presence of ultrasonics is ~3 times higher than that of the unused ultrasonic tool. This highlights the importance of the presence of ultrasonic waves in the photo-catalytic removal of ibuprofen. The rate of ibuprofen removal (k = 0.03 1/min) is similar to that reported for the Co_3O_4/BiOI visible light degradation (0.001–0.09 1/min) [13] and TiO_2-boron nitride nanocomposites (0.02–0.04 1/min) [46] systems. However, the testing conditions in our work and these reports are very different.

3.8. Pathway for ibuprofen degradation by the optimal catalyst

The products of ibuprofen decomposition caused by UV light, H_2O_2 oxidizer, and ultrasonic waves in the presence of photo-catalysts were investigated by GC-Mass (Fig. 9). It is expected that the hydroxyl radicals (OH·) created by UV light or ultrasonic waves will trigger the ibuprofen degradation reaction and alter the structure of the drug. Molecular structures based on the molecular weight of *m/z* obtained from the mass spectra were analyzed and plotted by Chem Draw software, the results of which are visible in Fig. 9. Proposed structures and pathways of destruction caused by ring-opening and methylation [47], oxidation [48], radical bond breakage [49], and sequential oxidation [50]. Similarly, lighter molecular weight fragments created by the degradation of ibuprofen in the developed system. Our results for the mass spectrum are supported by Fung and Ma et al. [51,52].

3.9. Proposed mechanism for ibuprofen degradation

The possible mechanism of the effect of zeolite-TiO_2 along with UV/Ultrasound/H_2O_2 for the decomposition of ibuprofen is shown in Fig. 10. At optimum pH (pH 5), elements such as Ti, Cl, Si, Ca, S, Al, Na, K, Zn, *etc.* in the zeolite structure are reacted with the pollutant and simultaneously the photo-catalyst with ultrasound results in the production of hydroxyl radical. Hydroxyl radicals are produced by photocatalysis and UV/ultrasound processes, which ultimately results in a collective effect and promotes the oxidation efficiency of ibuprofen (Eqs. 3–16). During these processes, the coupling of electrons and cavities at the TiO_2 surface is prevented, the mechanism being as TiO_2-stimulated photon electrons (due to UV radiation) are used to produce ions in the zeolite at lower capacities. The stoichiometric value of H_2O_2 consumption is calculated for ibuprofen mineralization in Eq. (2). It is expected that H_2O_2 will decompose to H· with ultrasound and generate more OH· [53,54]. Hydroxyl radicals can substantially degrade organic compounds, but often hydrogen peroxide is re-combined in large quantities with different rebels, reducing the rate of reaction [22,55]. [18,56]

$$C_{13}H_{18}O_2 + 33\ H_2O_2 \rightarrow 13\ CO_2 + 42\ H_2O \quad (3)$$

$$H_2O_2 \xrightarrow{Ultrasonicwaves} 2OH\bullet \quad (4)$$

$$H_2O_2 + H\cdot \rightarrow OH\cdot + H_2O \quad (5)$$

$$H_2O_2 + OH\cdot \rightarrow OOH\cdot + H_2O \quad (6)$$

$$OH\cdot + OH\cdot \rightarrow H_2O_2 \quad (7)$$

$$OH + H\cdot \rightarrow H_2O \quad (8)$$

$$OH\cdot + OOH\cdot \rightarrow H_2O + O_2 \quad (9)$$

$$OOH\cdot + OOH\cdot \leftrightarrow H_2O_2 + O_2 \quad (10)$$

$$OOH\cdot + H\cdot \rightarrow H_2O_2 \quad (11)$$

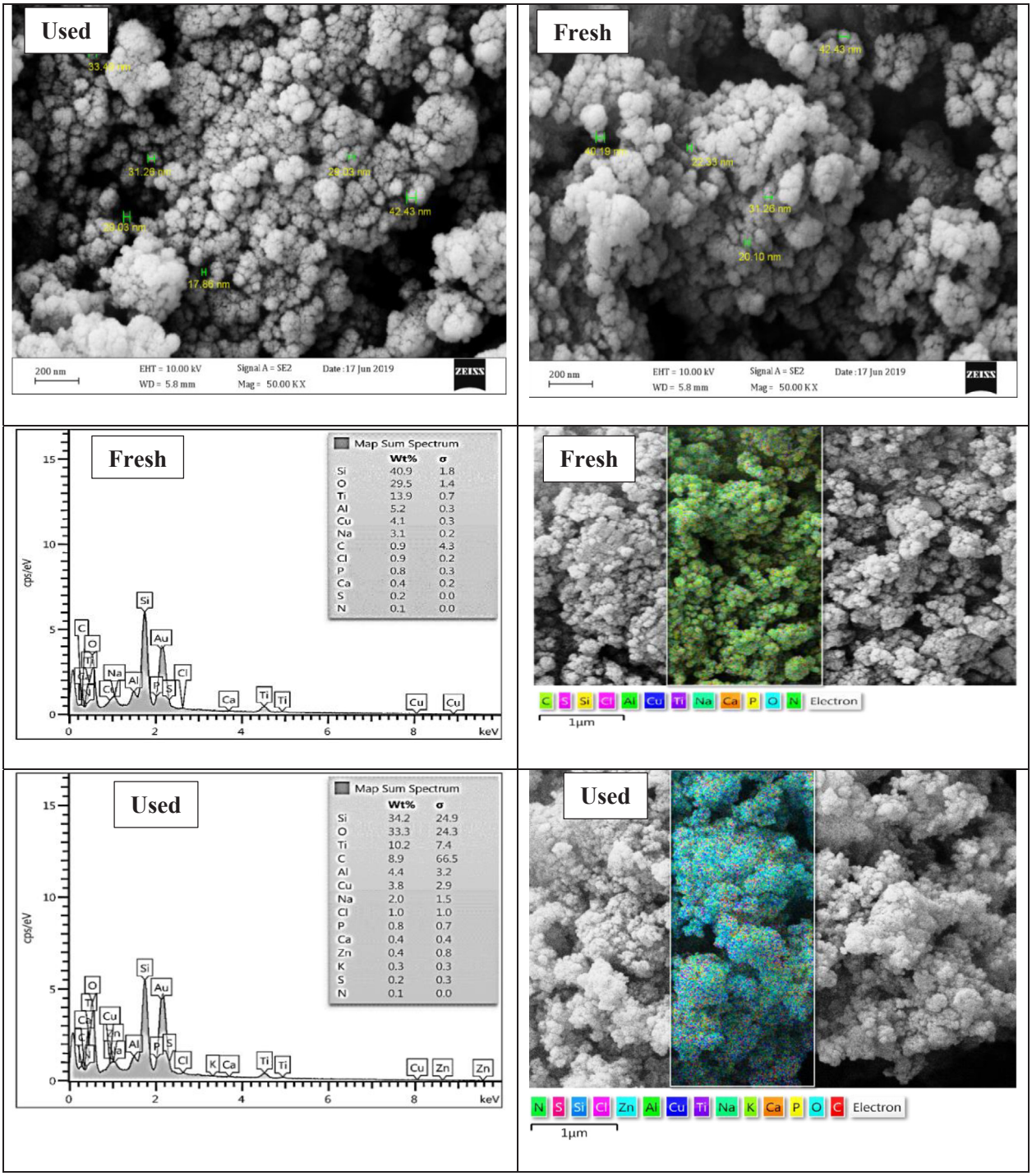

Fig. 7. SEM, EDX, and mapping for the fresh and used Cat-350-1-2 catalyst.

$$TiO_2\ (h^+) + Y \rightarrow TiO_2 + Y^+ \quad (12)$$

$$TiO_2\ (h^+) + H_2O \rightarrow TiO_2 + OH\cdot + H^+ \quad (14)$$

$$TiO_2\ (e^-) + O_2 \rightarrow TiO_2 + O^{2-} \quad (15)$$

$$TiO_2\ (e^-) + H_2O_2 \rightarrow TiO_2 + OH\cdot + OH^- \quad (16)$$

When the TiO_2 energy in the reaction suspension is even to or higher than the UV band gap the electron cavity pair can be generated. The excited photo-cavities are capable of accepting electrons present on the TiO_2 surface or in the solvent. This results in the oxidation of organic matter by the OH·, the photovoltaic, and O^- [28].

Hydroxyl radicals produced by ultrasonic waves (due to the pyrolytic decomposition of water molecules) are also useful in the drug removal process. The synergistic effect of sono-degradation with other advanced oxidation techniques removes many of the problems of sono-degradation in terms of energy consumption and time. The integration of advanced oxidation techniques with ultrasound increases the degradation rate and can be applied on a large scale [57,58].

The efficiency of the photolytic process can be significantly increased when UV radiation is combined with H_2O_2. The oxidizing power of H_2O_2 can be reasonably improved by generating HO by O-O splitting with sufficient quantum photon energy (~213 kJ/mol, at wavelength < 280 nm). During the use of UV/ H_2O_2, the rate of

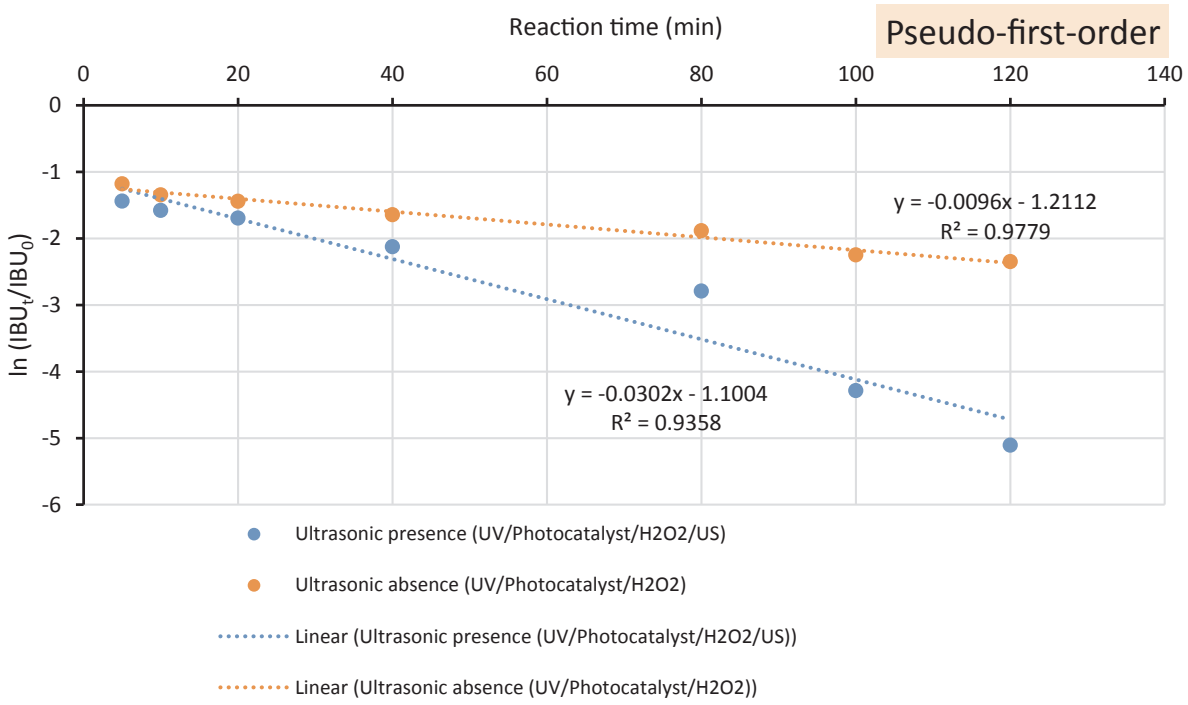

Fig. 8. Kinetic of the ibuprofen removal by the developed system in the presence/absence of ultrasonic wave (H_2O_2: 0.05 mM/L, pH: 5, UV power: 6 W, photocatalyst dose: 1.5 g/L).

degradation depends on the optimal oxidant concentration because it has a deterrent effect beyond it, and the radicals tend to recombine and reproduce H_2O_2 [21].

With the integrated system (zeolite-TiO_2-UV/ultrasound/H_2O_2), hydroxyl radicals are produced in large quantities in the reactor, thereby increasing the purification efficiency. Also, the electron-hole reconstitution in the photo-catalyst is reduced by this system, which increases the degradation efficiency. The excited electrons by ions in the photo-catalyst can block the electron reconstitution and, thus, the continuation of radical production [59].

3.10. Energy consumption in the presence/absence of ultrasonic wave

The energy consumed for the components of the ibuprofen removal system was calculated under optimal conditions (zeolite/TiO_2 dose: 0.07 g/ 150 mL, pH: 5, ibuprofen concentration: 100 mg/L, H_2O_2 dose: 0.7 mL, contact time: 100 min; UV power: 6 W). The amount of energy consumed for the zeolite-TiO_2-UV/ultrasound/H_2O_2 system as follows:

The voltage and electric current input to the ultrasonic device (Model S30H, Elma) was 230 V and 0.001 A, respectively. So, the power consumed per time unit by this device is:

- Supply voltage × Electric current = 230 V × 0.001 A = 0.23 J/s

Power consumption of the UV lamp per time unit is also computed as:

- Supply voltage × Electric current = 220 V × 0.03 A = 6.6 J/s

The IBU removal was done at 100 min sonication, so this time is equal to 6000 s (100 min × 60 s). The amount of electrical energy given to the solution in the reactor calculated using the calorimetric method and it was 5.04 kJ.

The value of energy consumed per 100 min sonication and UV exposure was determined as:

- 6000 s × 0.23 J/s × 6.6 J/s = 9.1 kJ

The values of consumed materials (water, H_2O_2, and photo-catalyst) in this study were 150.77 g. Therefore, the total amount of energy consumed per unit material was computed as:

- (9.1 kJ + 5.04 kJ)/ 150.77 g) = 0.094 kJ/g

The amount of energy consumed in 'sonication/H_2O_2/UV/zeolite-TiO_2' system for ibuprofen removal under optimal conditions was not significant (0.094 kJ/g). No article was found to compare the results.

If the sonication tool is not used to eliminate ibuprofen in the developed system (and instead of this tool the shaker-incubator is used), the energy consumption would be much higher (~17.5 kJ/g). This implies that the system used is economical.

4. Conclusion

This study aimed to develop a new sono-photocatalyst of zeolite-titanate to remove ibuprofen. The results showed that the zeolite-titanate nano-photocatalyst synthesized by the sol–gel way and calcined at 350 °C for two hours with a volume of 2 mL titanate (Cat-350-1-2) could be used as a viable option to remove ibuprofen from the aqueous phase. The optimal catalyst achieved the best degradation of IBU (89%) compared to other incentives in this study under similar conditions. The photocatalytic activity of the zeolite-titanate catalysts was strongly dependent on the calcination temperature. Short calcination time results in incomplete crystallization of titanate. In contrast, long calcination times result in burns, yellowing, and deformation of the crystals. The specific surface area of the optimal catalyst was 39 m^2/g and increased after being used in the IBU removal mainly due to ultrasonic waves. A comparison of XRD diffraction peaks revealed that the peak of titanium dioxide nanoparticles indicates the successful loading of the nanoparticles onto the zeolite material. The kinetics of drug removal in the presence and absence of ultrasonic waves differed significantly in terms of reaction rate. The system's energy consumption was calculated in the presence/absence of ultrasonic waves, indicating that the use of ultrasonic was more economically advantageous. In the end, the developed system is an effective and low-cost technique for the treatment

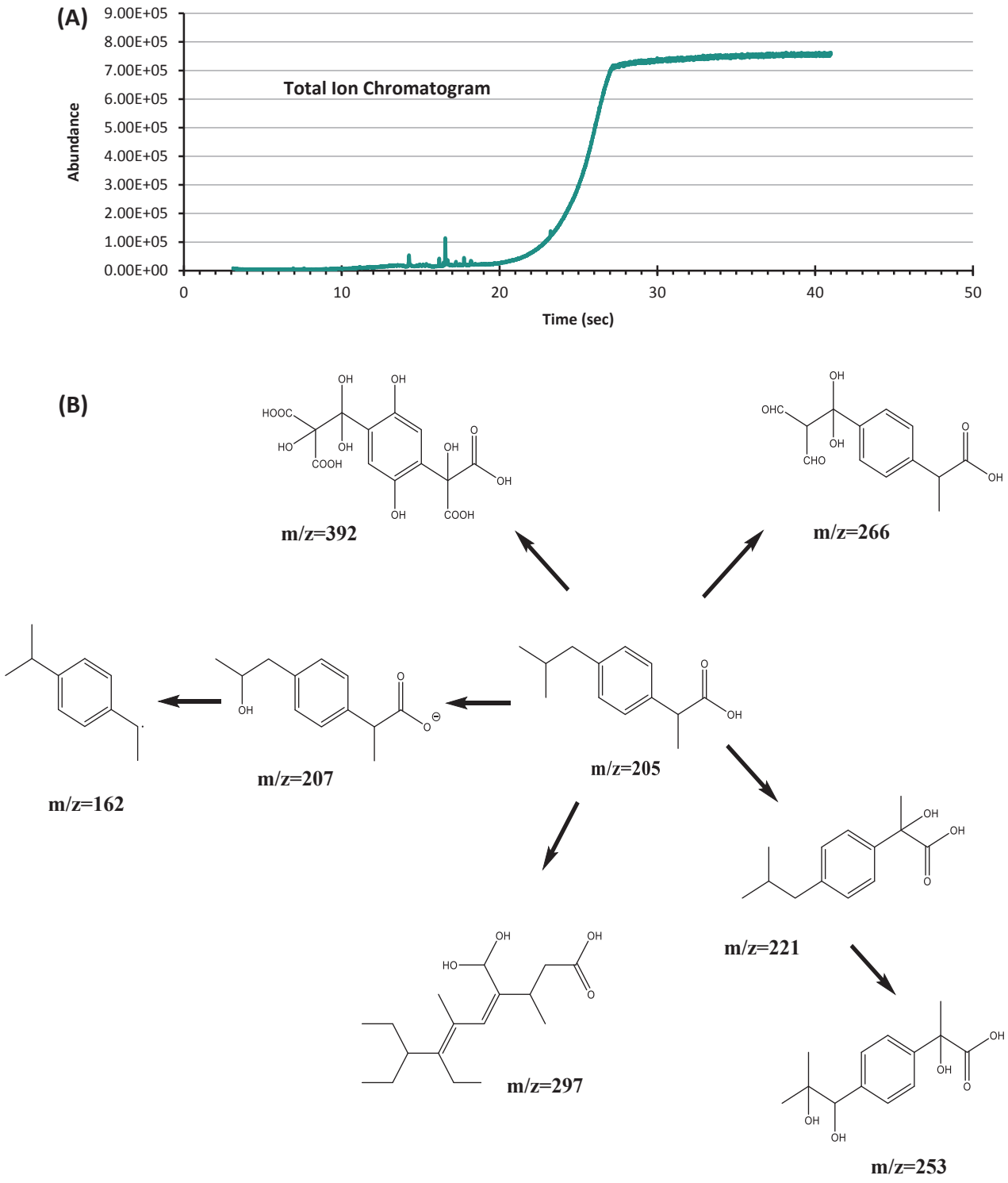

Fig. 9. (A) GC-mass graph for ibuprofen degradation by the developed system of "zeolite-titanate-H_2O_2-UV-ultrasonic" (B) degradation pathway of ibuprofen.

of wastewater containing ibuprofen.

CRediT authorship contribution statement

Narges Farhadi: Formal analysis, Writing - original draft. **Taybeh Tabatabaie:** Methodology, Conceptualization. **Bahman Ramavandi:** Supervision, Writing - review & editing. **Fazel Amiri:** Software, Validation.

Declaration of Competing Interest

The authors declare that they have no known competing financial interests or personal relationships that could have appeared to influence the work reported in this paper.

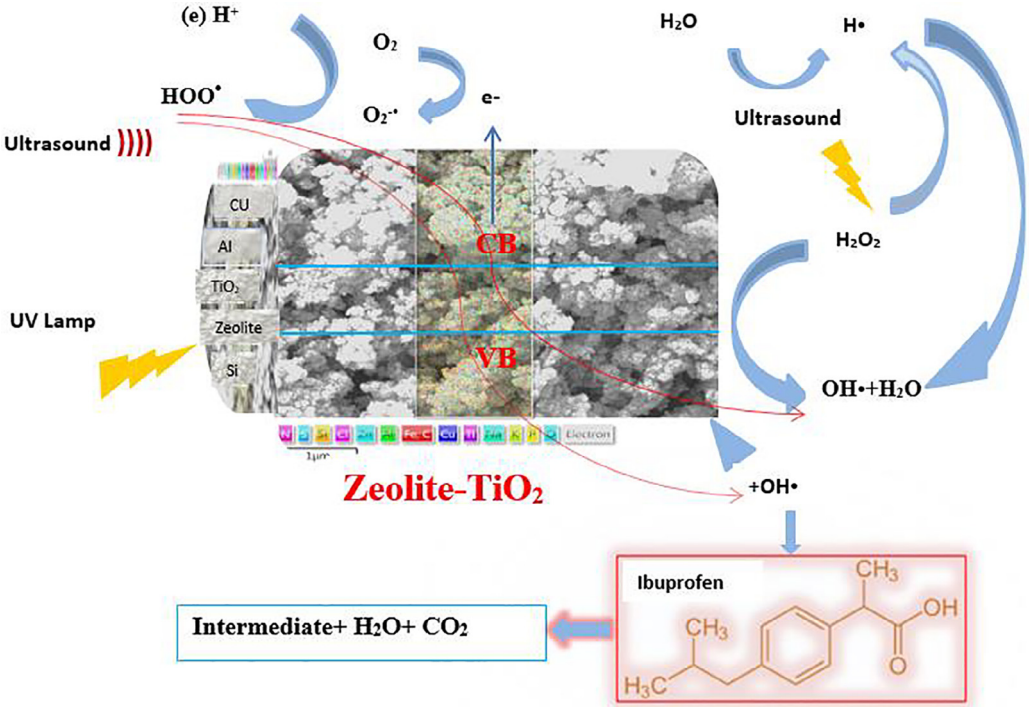

Fig. 10. The proposed mechanism for ibuprofen removal by the "Zeolite-titanium-H_2O_2-UV-ultrasonic" system.

Acknowledgements

The authors highly acknowledge the support of Iran High-Tech Laboratory Network for their help with catalyst characterization. The technical support of the Bushehr University of Medical Sciences is also acknowledged.

Appendix A. Supplementary data

Supplementary data to this article can be found online at https://doi.org/10.1016/j.ultsonch.2020.105122.

References

[1] F. Tavasol, T. Tabatabaie, B. Ramavandi, F. Amiri, Design a new photocatalyst of sea sediment/titanate to remove cephalexin antibiotic from aqueous media in the presence of sonication/ultraviolet/hydrogen peroxide: Pathway and mechanism for degradation, Ultrason. Sonochem. 105062 (2020).
[2] R. Davarnejad, B. Soofi, F. Farghadani, R. Behfar, Ibuprofen removal from a medicinal effluent: A review on the various techniques for medicinal effluents treatment, Environ. Technol. Innovation 11 (2018) 308–320.
[3] L. Feng, E.D. van Hullebusch, M.A. Rodrigo, G. Esposito, M.A. Oturan, Removal of residual anti-inflammatory and analgesic pharmaceuticals from aqueous systems by electrochemical advanced oxidation processes. A review, Chem. Eng. J. 228 (2013) 944–964.
[4] A. Ziylan, N.H. Ince, The occurrence and fate of anti-inflammatory and analgesic pharmaceuticals in sewage and fresh water: Treatability by conventional and non-conventional processes, J. Hazard. Mater. 187 (2011) 24–36.
[5] H. Guedidi, L. Reinert, Y. Soneda, N. Bellakhal, L. Duclaux, Adsorption of ibuprofen from aqueous solution on chemically surface-modified activated carbon cloths, Arab. J. Chem. 10 (2017) S3584–S3594.
[6] M. Ulfa, D. Prasetyoko, A.H. Mahadi, H. Bahruji, Size tunable mesoporous carbon microspheres using Pluronic F127 and gelatin as co-template for removal of ibuprofen, Sci. Total Environ. 711 (2020) 135066.
[7] A. Kruglova, P. Ahlgren, N. Korhonen, P. Rantanen, A. Mikola, R. Vahala, Biodegradation of ibuprofen, diclofenac and carbamazepine in nitrifying activated sludge under 12°C temperature conditions, Sci. Total Environ. 499 (2014) 394–401.
[8] L. Escuder-Gilabert, Y. Martín-Biosca, M. Perez-Baeza, S. Sagrado, M.J. Medina-Hernández, Direct chromatographic study of the enantioselective biodegradation of ibuprofen and ketoprofen by an activated sludge, J. Chromatogr. A 1568 (2018) 140–148.
[9] J. Madhavan, F. Grieser, M. Ashokkumar, Combined advanced oxidation processes for the synergistic degradation of ibuprofen in aqueous environments, J. Hazard. Mater. 178 (2010) 202–208.
[10] Z. Wang, V. Srivastava, I. Ambat, Z. Safaei, M. Sillanpää, Degradation of Ibuprofen by UV-LED/catalytic advanced oxidation process, J. Water Process Eng. 31 (2019) 100808.
[11] Q. Sun, X. Hu, S. Zheng, Z. Sun, S. Liu, H. Li, Influence of calcination temperature on the structural, adsorption and photocatalytic properties of TiO2 nanoparticles supported on natural zeolite, Powder Technol. 274 (2015) 88–97.
[12] M. Lim, Y. Zhou, B. Wood, Y. Guo, L. Wang, V. Rudolph, G. Lu, Fluorine and carbon codoped macroporous titania microspheres: highly effective photocatalyst for the destruction of airborne styrene under visible light, J. Phys. Chem. C 112 (2008) 19655–19661.
[13] M.E. Malefane, U. Feleni, P.J. Mafa, A.T. Kuvarega, Fabrication of direct Z-scheme Co3O4/BiOI for ibuprofen and trimethoprim degradation under visible light irradiation, Appl. Surf. Sci. 514 (2020) 145940.
[14] A. Pawlik, M. Jarosz, K. Syrek, G.D. Sulka, Co-delivery of ibuprofen and gentamicin from nanoporous anodic titanium dioxide layers, Colloids Surf., B 152 (2017) 95–102.
[15] S. Adityosulindro, C. Julcour, L. Barthe, Heterogeneous Fenton oxidation using Fe-ZSM5 catalyst for removal of ibuprofen in wastewater, J. Environ. Chem. Eng. 6 (2018) 5920–5928.
[16] M.A. Saepurahman, F.K. Abdullah, Chong, Dual-effects of adsorption and photo-degradation of methylene blue by tungsten-loaded titanium dioxide, Chem. Eng. J. 158 (2010) 418–425.
[17] S. Kong, Y. Wang, H. Zhan, M. Liu, L. Liang, Q. Hu, Competitive adsorption of humic acid and arsenate on nanoscale iron–manganese binary oxide-loaded zeolite in groundwater, J. Geochem. Explor. 144 (2014) 220–225.
[18] S. Adityosulindro, L. Barthe, K. González-Labrada, U.J. Jáuregui Haza, H. Delmas, C. Julcour, Sonolysis and sono-Fenton oxidation for removal of ibuprofen in (waste) water, Ultrason. Sonochem. 39 (2017) 889–896.
[19] M. Ondarts, L. Reinert, S. Guittonneau, S. Baup, S. Delpeux, J.-M. Lévêque, L. Duclaux, Improving the adsorption kinetics of ibuprofen on an activated carbon fabric through ultrasound irradiation: Simulation and experimental studies, Chem. Eng. J. 343 (2018) 163–172.
[20] M.J. Quero-Pastor, M.C. Garrido-Perez, A. Acevedo, J.M. Quiroga, Ozonation of ibuprofen: A degradation and toxicity study, Sci. Total Environ. 466–467 (2014) 957–964.
[21] I. Michael, Z. Frontistis, D. Fatta-Kassinos, Chapter 11 - Removal of Pharmaceuticals from Environmentally Relevant Matrices by Advanced Oxidation Processes (AOPs), in: M. Petrovic, D. Barcelo, S. Pérez (Eds.), Comprehensive Analytical Chemistry, Elsevier, 2013, pp. 345–407.
[22] F. Méndez-Arriaga, R.A. Torres-Palma, C. Pétrier, S. Esplugas, J. Gimenez, C. Pulgarin, Ultrasonic treatment of water contaminated with ibuprofen, Water Res. 42 (2008) 4243–4248.
[23] L. Jothinathan, J. Hu, Kinetic evaluation of graphene oxide based heterogenous catalytic ozonation for the removal of ibuprofen, Water Res. 134 (2018) 63–73.
[24] S. Suárez, I. Jansson, B. Ohtani, B. Sánchez, From titania nanoparticles to decahedral anatase particles: Photocatalytic activity of TiO2/zeolite hybrids for VOCs oxidation, Catal. Today 326 (2019) 2–7.
[25] F. Abdollah, S.M. Borghei, E. Moniri, S. Kimiagar, H.A. Panahi, Laser irradiation for controlling size of TiO < inf > 2 < /inf > -Zeolite nanocomposite in removal of 2,4-dichlorophenoxyacetic acid herbicide, Water Sci. Technol. 80 (2019) 864–873.

[26] N.U. Saqib, R. Adnan, I. Shah, Zeolite supported TiO < inf > 2 < /inf > with enhanced degradation efficiency for organic dye under household compact fluorescent light, Mater. Res. Express 6 (2019).
[27] A.P. Aziztyana, S. Wardhani, Y.P. Prananto, D. Purwonugroho, Darjito, optimisation of methyl orange photodegradation using TiO < inf > 2 < /inf > -zeolite photocatalyst and H < inf > 2 < /inf > O < inf > 2 < /inf > in Acid Condition, IOP Conference Series: Materials Science and Engineering, (2019).
[28] X. Liu, Y. Liu, S. Lu, W. Guo, B. Xi, Performance and mechanism into TiO2/Zeolite composites for sulfadiazine adsorption and photodegradation, Chem. Eng. J. 350 (2018) 131–147.
[29] E. Dauksta, A. Medvids, P. Onufrijevs, M. Shimomura, Y. Fukuda, K. Murakami, Laser-induced crystalline phase transition from rutile to anatase of niobium doped TiO2, Curr. Appl Phys. 19 (2019) 351–355.
[30] T. Kaur, A. Sraw, R.K. Wanchoo, A.P. Toor, Solar assisted degradation of carbendazim in water using clay beads immobilized with TiO2 & Fe doped TiO2, Sol. Energy 162 (2018) 45–56.
[31] J. de Clermont-Gallerande, S. Saito, T. Hayakawa, M. Colas, J.-R. Duclère, P. Thomas, Optical properties of Nd3 + -doped TeO2-TiO2-ZnO glasses with lower hydroxyl content, J. Non-Cryst. Solids 528 (2020) 119678.
[32] S. Gomez, C.L. Marchena, L. Pizzio, L. Pierella, Preparation and characterization of TiO2/HZSM-11 zeolite for photodegradation of dichlorvos in aqueous solution, J. Hazard. Mater. 258–259 (2013) 19–26.
[33] M. Pelaez, P. Falaras, V. Likodimos, A.G. Kontos, A.A. de la Cruz, K. O'Shea, D.D. Dionysiou, Synthesis, structural characterization and evaluation of sol–gel-based NF-TiO2 films with visible light-photoactivation for the removal of microcystin-LR, Appl. Catal. B 99 (2010) 378–387.
[34] N. Lu, H.T. Yu, Y. Su, Y. Wu, Water absorption and photocatalytic activity of TiO2 in a scrubber system for odor control at varying pH, Sep. Purif. Technol. 90 (2012) 196–203.
[35] J. Cai, W. Xin, G. Liu, D. Lin, D. Zhu, Effect of calcination temperature on structural properties and photocatalytic activity of Mn-C-codoped TiO2, Mater. Res. 19 (2016) 401–407.
[36] F. Yaripour, Z. Shariatinia, S. Sahebdelfar, A. Irandoukht, Effect of boron incorporation on the structure, products selectivities and lifetime of H-ZSM-5 nanocatalyst designed for application in methanol-to-olefins (MTO) reaction, Microporous Mesoporous Mater. 203 (2015) 41–53.
[37] G. Liu, S. Liao, D. Zhu, J. Cui, W. Zhou, Solid-phase photocatalytic degradation of polyethylene film with manganese oxide OMS-2, Solid State Sci. 13 (2011) 88–94.
[38] R. Khosravi, A. Zarei, M. Heidari, A. Ahmadfazeli, M. Vosughi, M. Fazlzadeh, Application of ZnO and TiO2 nanoparticles coated onto montmorillonite in the presence of H2O2 for efficient removal of cephalexin from aqueous solutions, Korean J. Chem. Eng. 35 (2018) 1000–1008.
[39] K.K. Kefeni, B.B. Mamba, Photocatalytic application of spinel ferrite nanoparticles and nanocomposites in wastewater treatment: Review, Sustainable Mater.Technol. 23 (2020) e00140.
[40] S.H. Sonawane, B.A. Bhanvase, A.A. Jamali, S.K. Dubey, S.S. Kale, D.V. Pinjari, R.D. Kulkarni, P.R. Gogate, A.B. Pandit, Improved active anticorrosion coatings using layer-by-layer assembled ZnO nanocontainers with benzotriazole, Chem. Eng. J. 189–190 (2012) 464–472.
[41] M.-S. Miao, Q. Liu, L. Shu, Z. Wang, Y.-Z. Liu, Q. Kong, Removal of cephalexin from effluent by activated carbon prepared from alligator weed: Kinetics, isotherms, and thermodynamic analyses, Process Saf. Environ. Prot. 104 (2016) 481–489.
[42] G. Liao, W. Yao, J. Zuo, Preparation and characterization of zeolite/TiO_2 cement-based composites with excellent photocatalytic performance, Materials (Basel) 11 (2018) 2485.
[43] T. Wan, W. Cheng, W.J. Shi, J.H. Ren, W. Wu, J. Yao, Photocatalytic degradation of sulfamonomethoxine in aqueous phase using PW12/TiO2 composites under UV lights, IOP Conf. Series: Earth Environ. Sci. 191 (2018) 012039.
[44] Y.A.J. Al-Hamadani, C.M. Park, L.N. Assi, K.H. Chu, S. Hoque, M. Jang, Y. Yoon, P. Ziehl, Sonocatalytic removal of ibuprofen and sulfamethoxazole in the presence of different fly ash sources, Ultrason. Sonochem. 39 (2017) 354–362.
[45] M. Gągol, A. Przyjazny, G. Boczkaj, Wastewater treatment by means of advanced oxidation processes based on cavitation – A review, Chem. Eng. J. 338 (2018) 599–627.
[46] L. Lin, W. Jiang, M. Bechelany, M. Nasr, J. Jarvis, T. Schaub, R.R. Sapkota, P. Miele, H. Wang, P. Xu, Adsorption and photocatalytic oxidation of ibuprofen using nanocomposites of TiO2 nanofibers combined with BN nanosheets: Degradation products and mechanisms, Chemosphere 220 (2019) 921–929.
[47] H. Cy, F. Lh, S. Mh, H. Cf, W. Jp, K. Hw, Ibuprofen biodegradation by hospital, municipal, and distillery activated sludges, Environ. Technol 41 (2020) 171–180.
[48] J. Rodríguez-Chueca, C. Garcia-Cañibano, M. Sarro, Á. Encinas, C. Medana, D. Fabbri, P. Calza, J. Marugán, Evaluation of transformation products from chemical oxidation of micropollutants in wastewater by photoassisted generation of sulfate radicals, Chemosphere 226 (2019) 509–519.
[49] S. Li, Z. Wang, X. Zhang, J. Zhao, Z. Hu, Z. Wang, X. Xie, Preparation of magnetic nanosphere/nanorod/nanosheet-like Fe3O4/Bi2S3/BiOBr with enhanced (0 0 1) and (1 1 0) facets to photodegrade diclofenac and ibuprofen under visible LED light irradiation, Chem. Eng. J. 378 (2019) 122169.
[50] R. Salgado, D. Brito, J.P. Noronha, B. Almeida, M.R. Bronze, A. Oehmen, G. Carvalho, M.T. Barreto Crespo, Metabolite identification of ibuprofen biodegradation by Patulibacter medicamentivorans under aerobic conditions, Environ. Technol. 41 (2020) 450–465.
[51] C.S.L. Fung, M. Khan, A. Kumar, I.M.C. Lo, Visible-light-driven photocatalytic removal of PPCPs using magnetically separable bismuth oxybromo-iodide solid solutions: Mechanisms, pathways, and reusability in real sewage, Sep. Purif. Technol. 216 (2019) 102–114.
[52] M. Ma, L. Chen, J. Zhao, W. Liu, H. Ji, Efficient activation of peroxymonosulfate by hollow cobalt hydroxide for degradation of ibuprofen and theoretical study, Chin. Chem. Lett. 30 (2019) 2191–2195.
[53] P.R. Gogate, Treatment of wastewater streams containing phenolic compounds using hybrid techniques based on cavitation: A review of the current status and the way forward, Ultrason. Sonochem. 15 (2008) 1–15.
[54] A.M. Lastre-Acosta, G. Cruz-Gonzalez, L. Nuevas-Paz, U.J. Jauregui-Haza, A.C. Teixeira, Ultrasonic degradation of sulfadiazine in aqueous solutions, Environ. Sci. Pollut. Res. Int. 22 (2015) 918–925.
[55] E. Neyens, J. Baeyens, A review of classic Fenton's peroxidation as an advanced oxidation technique, J. Hazard. Mater. 98 (2003) 33–50.
[56] P. Bansal, A. Verma, Synergistic effect of dual process (photocatalysis and photo-Fenton) for the degradation of Cephalexin using TiO2 immobilized novel clay beads with waste fly ash/foundry sand, J. Photochem. Photobiol., A 342 (2017) 131–142.
[57] B. Thokchom, P. Qiu, M. Cui, B. Park, A.B. Pandit, J. Khim, Magnetic Pd@Fe3O4 composite nanostructure as recoverable catalyst for sonoelectrohybrid degradation of Ibuprofen, Ultrason. Sonochem. 34 (2017) 262–272.
[58] N.H. Ince, Ultrasound-assisted advanced oxidation processes for water decontamination, Ultrason. Sonochem. 40 (2018) 97–103.
[59] F. Mazille, T. Schoettl, C. Pulgarin, Synergistic effect of TiO2 and iron oxide supported on fluorocarbon films. Part 1: Effect of preparation parameters on photocatalytic degradation of organic pollutant at neutral pH, Appl. Catal. B 89 (2009) 635–644.